PNAS RESEARCH ARTICLE | IMMUNOLOGY AND INFLAMMATION

Nitro-oleic acid regulates T cell activation through post-translational modification of calcineurin

Ángel Bago[a], M. Laura Cayuela[a], Alba Gil[a], Enrique Calvo[b,c], Jesús Vázquez[b,c], Antonio Queiro[d], Francisco J. Schopfer[e], Rafael Radi[f,g], Juan M. Serrador[a,1,2], and Miguel A. Íñiguez[a,h,i,j,1,2]

Edited by George Kokotos, Department of Chemistry, Ethniko kai Kapodistriako Panepistemio Athenon, Greece; received May 24, 2022; accepted December 10, 2022 by Editorial Board Member Philippa Marrack

Nitro-fatty acids (NO_2-FAs) are unsaturated fatty acid nitration products that exhibit anti-inflammatory actions in experimental mouse models of autoimmune and allergic diseases. These electrophilic molecules interfere with intracellular signaling pathways by reversible post-translational modification of nucleophilic amino-acid residues. Several regulatory proteins have been identified as targets of NO_2-FAs, modifying their activity and promoting gene expression changes that result in anti-inflammatory effects. Herein, we report the effects of nitro-oleic acid (NO_2-OA) on pro-inflammatory T cell functions, showing that 9- and 10-NOA, but not their oleic acid precursor, decrease T cell proliferation, expression of activation markers CD25 and CD71 on the plasma membrane, and IL-2, IL-4, and IFN-γ cytokine gene expressions. Moreover, we have found that NO_2-OA inhibits the transcriptional activity of nuclear factor of activated T cells (NFAT) and that this inhibition takes place through the regulation of the phosphatase activity of calcineurin (CaN), hindering NFAT dephosphorylation, and nuclear translocation in activated T cells. Finally, using mass spectrometry-based approaches, we have found that NO_2-OA nitroalkylates CaNA on four Cys (Cys129, 228, 266, and 372), of which only nitroalkylation on Cys372 was of importance for the regulation of CaN phosphatase activity in cells, disturbing functional CaNA/CaNB heterodimer formation. These results provide evidence for an additional mechanism by which NO_2-FAs exert their anti-inflammatory actions, pointing to their potential as therapeutic bioactive lipids for the modulation of harmful T cell-mediated immune responses.

nitro-fatty acids | T cells | NFAT | calcineurin | inflammation

Significance

In addition to maintaining the fluidity of the plasma membrane, some unsaturated fatty acids are involved in signal transduction. Inflammatory environments enhance the reaction of these lipids with nitrogen-derived reactive species to form electrophilic nitro-fatty acids (NO_2-FAs) that display increased reactivity toward cellular nucleophiles. By selective nitroalkylation of Cys residues on key signaling regulatory proteins, NO_2-FAs exert effective anti-inflammatory actions in some preclinical animal models of autoimmunity and allergy. Here we have identified the Ser/Thr phosphatase calcineurin as a new target of nitroalkylation by nitro-oleic acid. The nitroalkylation of calcineurin on Cys372 reduces the transcriptional activity of NFAT and modulates pro-inflammatory cytokine production by activated T cells. Our results underscore how NO_2-FAs may control T cell-mediated immune responses.

Nitro-fatty acids (NO_2-FAs), such as nitro-oleic acid (NO_2-OA), are electrophilic endogenous signaling molecules detected in human urine and plasma (1, 2). Under pathophysiological conditions, the reaction of nitric oxide-derived nitrogen reactive species such as nitrogen dioxide (NO_2) and peroxynitrite ($OONO^-$) with unsaturated and conjugated FAs leads to the increased formation of NO_2-FAs (3). Different mechanisms have been reported for the biological actions of these molecules; however, electrophilic nitroalkylation of Cys and, to a lower extent, of His, is central to their signaling activities. This reversible post-translational modification (PTM) can modify protein structure, function, and localization (4). Functional consequences of protein nitroalkylation have been shown in multiple biological systems. Targets of nitroalkylation include transcription factors such as peroxisome proliferator-activated receptor (PPAR)-γ (5), Kelch-like ECH-associated protein 1 (Keap1) (6), signal transducer and activator of transcription (STAT)-3 (7), and nuclear factor κB (NF-κB) (8), resulting in increased expression of antioxidant response genes and downregulation of NF-κB-dependent pro-inflammatory cytokines, mechanisms by which NO_2-FA exert many of their cytoprotective and anti-inflammatory actions (9–11). In addition, there is increasing evidence suggesting that these molecules might also be effective modulators of the immune response. The activation of macrophages, leukocyte tissue infiltration, and induction of pro-inflammatory cytokines and chemokines such as interleukin (IL)-6, tumor necrosis factor (TNF)-α, or monocyte chemoattractant protein-1 are attenuated by NO_2-OA (12). Moreover, the administration of NO_2-OA exerts protective effects on a wide range of experimental animal models of chronic inflammation where T lymphocytes and the activation of the immune system play a key role, such as psoriasis, inflammatory arthritis, allergic airway disease, allergic contact dermatitis, atherosclerosis, lung injury, and inflammatory bowel disease (7, 13–20). The therapeutic activity in preclinical animal models has led to the clinical development of 10-NO_2-OA (10NOA, developed as CXA-10) as an anti-inflammatory drug (21). Even though considerable evidence exists about the beneficial role of NO_2-FAs in the

This article is a PNAS Direct Submission. G.K. is a guest editor invited by the Editorial Board.

[1]J.M.S. and M.A.Í. contributed equally to this work and share coseniorship.

[2]To whom correspondence may be addressed. Email: jmserrador@cbm.csic.es or miguelangel.inniguez@uam.es.

This article contains supporting information online at https://www.pnas.org/lookup/suppl/doi:10.1073/pnas.2208924120/-/DCSupplemental.

Published January 18, 2023.

development and progression of chronic inflammation in autoimmune and allergic diseases, little is known about their underlying mechanisms of action and whether those may take place through the regulation of T cell functions.

To become functionally competent, T cells require a complex antigen-dependent cascade of events triggered by the T cell receptor (TCR), leading to the activation of transcription factors and expression of activation-induced genes that regulate cell proliferation, differentiation, and acquisition of effectors functions (22, 23). Among these transcription factors, nuclear factor of activated T cell (NFAT) proteins are particularly relevant, being involved in the regulation of the transcriptional induction of genes that are essential for the immune and inflammatory response such as cytokines (IL-2, IL-4, Interferon (IFN)-γ, IL-13, Granulocyte macrophage colony-stimulating factor, TNF-α) and cell surface receptors (CD25, FasL, CD40L) (24, 25).

Here, focusing on the study of NO_2-OA as a pharmacological agent with proven therapeutic efficacy in some experimental animal models of autoimmunity and allergy, but whose mechanisms of action on this group of diseases are still largely unknown, we explore whether some of their immunomodulatory actions may take place through the regulation of T cell functions. To address this, we have compared the activation and proliferation of human T lymphocytes treated with NO_2-OA or its unsaturated fatty acid precursor. We provide evidence that NO_2-OA interferes with T cell activation and function by modulating gene expression at the transcriptional level. We demonstrate that electrophilic NO_2-OA decreases NFAT dephosphorylation and nuclear translocation, impairing TCR-triggered transcriptional induction of IL-2, IL-4, and IFN-γ. Moreover, we have found that NO_2-OA inhibits NFAT through nitroalkylation of functionally-significant cysteines on the calcineurin (CaN) catalytic subunit A (CaNA), which disturbs CaNA/CaNB heterodimer formation and phosphatase function, revealing the importance of NO_2-FA-derived PTMs for the modulation of T cell-dependent immune responses.

Results

NO_2-OA Impairs T Cell Activation and Cytokine Production. To explore whether NO_2-OA regulates T cell activation, the effects of the NO_2-OA positional isomers 9NOA and 10NOA, respectively on the induction of the IL-2R α-chain CD25, the transferrin receptor CD71, and the very early activation inducer molecule CD69 (26), were compared with those of their oleic acid (OA) precursor. Changes in the upregulation of these activation markers on primary human T lymphoblasts stimulated via the TCR with CD3 agonistic antibodies (Abs) and the co-stimulatory molecule CD28, were analyzed by flow cytometry. Dose–response assays showed that, while OA did not change the expression levels of CD25, both 9NOA and 10NOA reduced the percentage of cells positive for CD25 and their median fluorescence intensity ratios (MFIR) in a dose-dependent fashion (Fig. 1*A*), reaching an IC50 of approximately 5 μM. Both NO_2-FAs also reduced the activation-mediated induction of membrane expression of CD71, but not of CD69 (Fig. 1*B*). Moreover, kinetic studies showed that the inhibitory effect exerted by 5 μM 10NOA on the expression of CD25 continued for at least 36 h (*SI Appendix*, Fig. S1), suggesting that in these cells 10NOA may affect late TCR-triggered events. We next analyzed whether NO_2-OA was able to inhibit activation-induced T cell proliferation. Human peripheral blood $CD4^+$ and $CD8^+$ T lymphocytes were loaded with the fluorescent probe Cell Trace Violet, and the proliferation was determined by flow cytometry after stimulation via CD3/CD28 in the presence of 10NOA or OA. The pretreatment of $CD4^+$ and $CD8^+$ T lymphocytes with 10NOA significantly diminished their proliferative response to CD3/CD28 stimulation, compared with non-treated cells or cells treated with OA (Fig. 1*C*). The anti-proliferative actions exerted by NO_2-OA were not related to cytotoxic or pro-apoptotic effects, as 10NOA barely affected the viability of T lymphocytes (*SI Appendix*, Fig. S2).

Since IL-2 is an essential autocrine growth factor for T cell survival and expansion, we next studied whether NO_2-OA affected IL-2 production. Interestingly, we found that both 9NOA and 10NOA significantly reduced the levels of IL-2 secreted by T lymphocytes in response to TCR-triggered activation (Fig. 1*D*). To investigate whether NO_2-OA regulates other cytokines in T cells, IFN-γ-producing Th1, and IL-4-producing Th2 cells were activated with a combination of phorbol 12-myristate 13-acetate (PMA) plus ionomycin, and treated with OA, 10NOA or the immunosuppressant agent CsA. Upon stimulation with PMA/ionomycin, approximately half of Th1 cells and a fifth of Th2 cells expressed IFN-γ (Fig. 1*E*) and IL-4 (Fig. 1*F*), respectively. Interestingly, 10NOA but not OA, reduced by half the number of cells expressing IFN-γ and lowered the production of IL-4 somewhat further, mirroring the effects observed in cells treated with CsA (Fig. 1 *E* and *F*).

NO_2-OA Inhibits IL-2, IFN-γ, and IL-4 Production at the Transcriptional Level. To assess whether NO_2-OA decreased cytokine production at the transcriptional level, IL-2, IFN-γ, and IL-4 mRNA levels in resting and CD3/CD28-stimulated human T lymphoblasts pretreated or not with 10NOA, were studied by RT-qPCR. In these cells, 10NOA reduced the induction of IL-2, IFN-γ, and IL-4 mRNAs in response to TCR-triggered activation (Fig. 2*A*). To investigate whether 10NOA reduced cytokine mRNA expression by interfering with gene transcriptional activation, Jurkat T cells were transfected with luciferase reporter plasmids containing promoter region constructs of IL-2, IFN-γ, or IL-4 genes, and stimulated with PMA plus calcium ionophore A23187 (Ion) in the presence or not of NO_2-OA or OA. The increase in IL-2, IFN-γ, and IL-4 promoter activities in response to stimulation with PMA/Ion was reduced by both 9NOA and 10NOA, but not by OA treatment (Fig. 2*B*).

These results demonstrate that, in T lymphocytes, NO_2-OA regulates TCR-triggered cytokine production at the transcriptional level, suggesting a mechanism that involves inhibition of common activation-induced signals responsible for transcriptional expression of IL-2, IFN-γ, and IL-4 genes.

NO_2-OA Interferes with NFAT-Mediated Transcriptional Activity. NF-κB, NFAT, and activator protein 1 (AP-1) have long been considered essential transcription factors for cytokine synthesis in T lymphocytes activated in response to antigen recognition (27). Since DNA regulatory elements for the binding of these transcription factors are consistently present in the promoter regions of IL-2, IFN-γ, and IL-4, we studied whether NO_2-OA could reduce cytokine synthesis by interfering with activation of some of these transcription factors. To evaluate the effect of NO_2-OA on NF-κB-mediated transcription in T lymphocytes, TCR Vβ3-expressing CH7C17 Jurkat cells were transfected with a luciferase reporter plasmid containing three tandem repeats of a consensus NF-κB-binding site (pNFκB-Luc). These cells were pretreated or not with NO_2-OA or OA and stimulated with Staphylococcal enterotoxin B superantigen (SEB)-pulsed antigen-presenting cells (APC) of the Raji B cell line or with PMA/Ion. NF-κB-dependent transcriptional activity increased in Jurkat cells upon stimulation with either

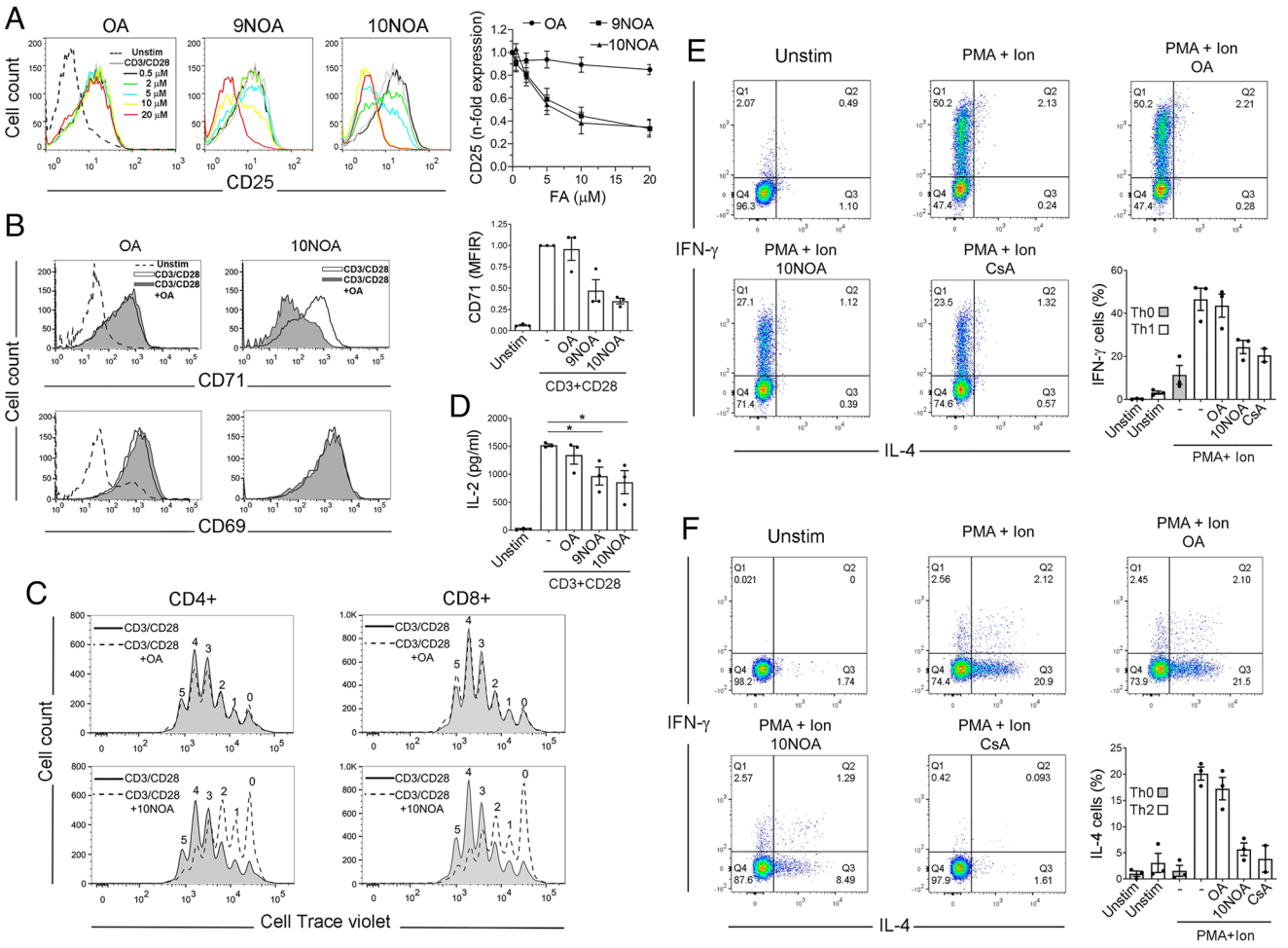

Fig. 1. NO_2-OA Reduces T Cell Proliferation, Expression of Activation Markers and Cytokine Production. (*A*) Flow cytometry analysis of CD25 expression on the cell surface of primary human T lymphoblasts unstimulated (dashed line) or stimulated with CD3/CD28 Abs for 12 h in the presence of different concentrations of OA, 9NOA or 10NOA (0.5 to 20 μM) (continuous lines). On the right, the corresponding fluorescence intensity ratios (MFIR) (mean ± SEM) for each treatment and concentration from four independent experiments are plotted. (*B*) Flow cytometry analysis of CD71 and CD69 cell surface expression in the presence of OA, 9NOA or 10NOA (5 μM). On the right, CD71 MFIR (mean ± SEM) from three independent experiments are depicted. (*C*) Cell Trace-Violet-labeled $CD4^+$ and $CD8^+$ T cells were stimulated with CD3/CD28 Abs for 6 d in the presence or absence of OA or 10NOA (5 μM) and proliferation was analyzed by flow cytometry. The figure shows $CD4^+$ and $CD8^+$ T cells that have divided one to five times based on Cell Trace-Violet dilution peaks. (*D*) ELISA determinations of IL-2 released to the culture medium of T cell stimulated for 16 h with CD3/CD28 Abs in the presence of OA or 10NOA (5 μM). *$P < 0.05$. (*E* and *F*) Dot plot flow cytometry analysis of IL-4 and IFN-γ intracellular staining in Th1 (*E*) and Th2 (*F*) cells activated for 6 h with PMA (15 ng/mL) plus ionomycin (Ion) (1 μM) in the presence of OA (5 μM), 10NOA (5 μM) or CsA (250 ng/mL). Percentage of negative cells, IL-4^+ and/or IFN-γ^+ cells are indicated in each quadrant (Q4-1). A representative experiment is shown. On the lower right corner of (*E*) and (*F*), histograms represent the percentage of IFN-γ^+ Th1 cells and IL4^+ Th2 cells (mean ± SEM) from three independent experiments. Results with non-differentiated Th0 cells are also shown.

SEB-pulsed APC or PMA/Ion. Interestingly, cell pretreatment with NO_2-OA significantly reduced NF-κB transcriptional activity, whereas OA did not show any effect (*SI Appendix*, Fig. S3*A*). Moreover, NO_2-OA reduced the phosphorylation of inhibitor of κB (IκB) and increased its stabilization in Jurkat cells stimulated with PMA/Ion (*SI Appendix*, Fig. S3*B*). Notably, NO_2-OA exerted similar effects on NFAT activity. As shown in Fig. 3*A*, NO_2-OA, but not OA, reduced NFAT-dependent transcriptional activity in Jurkat cells transfected with a luciferase reporter plasmid containing three tandem copies of the distal NFAT site of the human IL-2 promoter (pNFAT-Luc) and stimulated with either SEB or PMA/Ion. Since pNFAT-Luc contained synergistic AP-1-binding DNA consensus sequences, we next studied whether NO_2-OA was actually targeting NFAT. For this purpose, the effect of NO_2-OA on the transcriptional activity of a specific AP-1-Luc reporter plasmid was studied in Jurkat cells stimulated with PMA/Ion. Results showed that neither OA nor NO_2-OA affected the induction of AP-1-dependent transcriptional activity (Fig. 3*B*). NO_2-OA-induced inhibition of NFAT-dependent transcription was confirmed by the analysis of the promoter activity and protein expression of the RCAN1 gene, whose transcription is highly dependent on NFAT (28). The activity of a luciferase reporter plasmid under the regulation of the gene promoter region of RCAN1 (pRCAN1-Luc) increased in Jurkat cells upon stimulation with PMA/Ion, and either 9NOA or 10NOA, but not OA, abrogated this effect (Fig. 3*C*). Moreover, western blot analyses carried out in parallel showed that inducible RCAN1.4 but not constitutive RCAN1.1 protein levels increased in Jurkat cells in response to the stimulation with PMA/Ion and were reduced by cell pretreatment with 10NOA or CsA, but not OA (Fig. 3*D*), supporting that NO_2-OA inhibits NFAT-dependent transcriptional gene expression in activated T cells.

NO_2-OA Decreases NFAT Activation. The translocation of NFAT from the cytoplasm to the nucleus depends on CaN-mediated

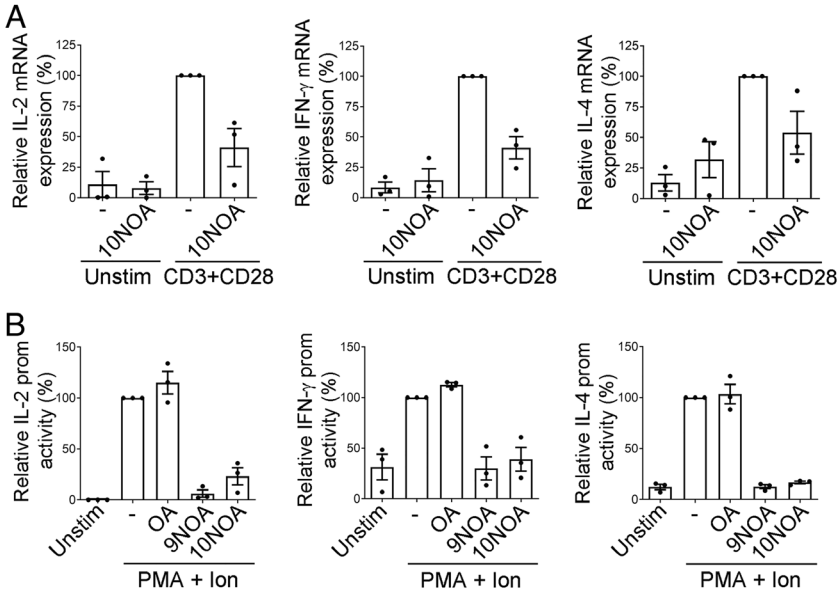

Fig. 2. NO_2-OA Reduces Transcriptional Induction of Cytokine Gene Expression in T Lymphocytes. (*A*) RT–qPCR analysis of IL-2, IFN-γ and IL-4 mRNA levels in human T lymphoblasts stimulated with CD3/CD28 Abs for 6 h in the presence or absence of 10NOA (5 μM). Results are represented as percentages with respect to CD3+CD28 stimulated T cells (mean ± SEM) of three independent experiments performed in triplicate. (*B*) Jurkat T cells transfected with IL-2, IFN-γ, or IL-4 promoter luciferase reporter plasmids were left unstimulated or treated for 6 h with PMA (15 ng/mL) plus calcium ionophore A23187 (Ion) (1 μM) in the absence or presence of OA, 9NOA or 10NOA (5 μM). IL2, IFN-γ, and IL-4 promoter transcriptional activities are represented as percentages of induction (observed RLU/basal RLU) with respect to CD3+CD28 stimulated T cells (mean ± SEM) of three independent experiments performed in triplicate.

dephosphorylation of conserved phosphoserines within the regulatory N-terminal region of NFAT. This is a critical step in the NFAT activation pathway that allows the specific interaction between this transcription factor and its corresponding response elements in the promoter region of many cytokine genes (29, 30). To assess whether NO_2-OA inhibits transcriptional activity of

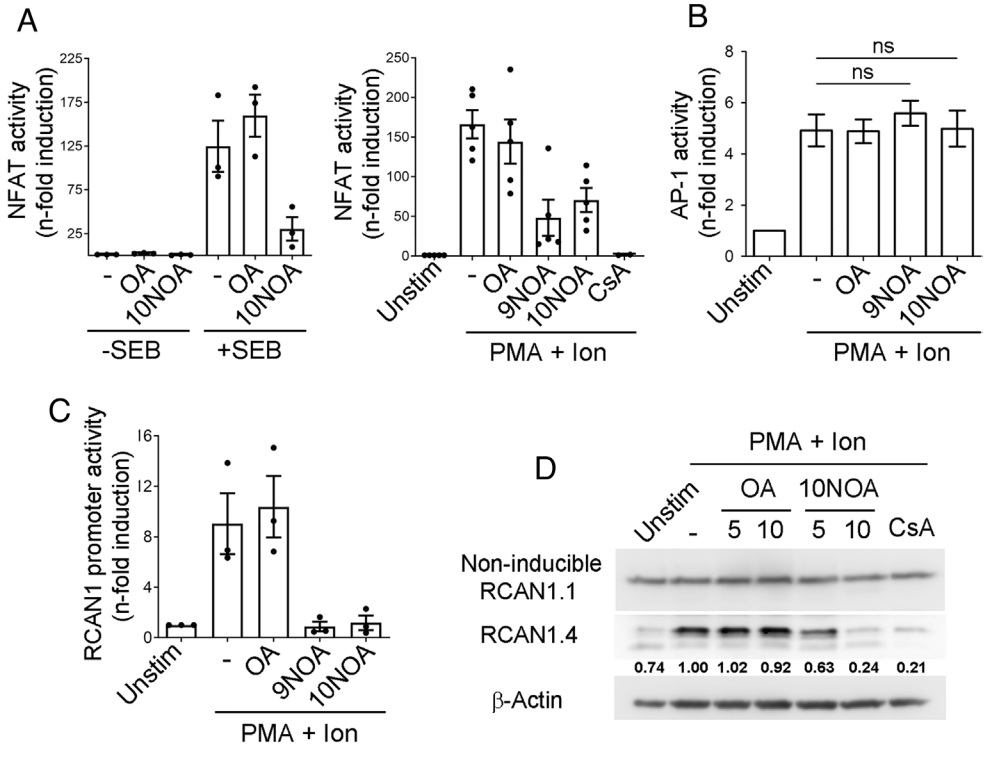

Fig. 3. NO_2-OA Reduces NFAT-Mediated Transcriptional Activity in T Lymphocytes. (*A–C*) Jurkat cells were transiently transfected with luciferase reporter constructs containing response elements for transcription factors NFAT (pNFAT-LUC), AP-1 (pAP-1-LUC) or the promoter region of RCAN1 (pRCAN1-LUC) and pretreated or not with OA, 9NOA, 10NOA (5 μM) or CsA (250 ng/mL), as indicated, before stimulation with superantigen B (SEB)-pulsed Raji B cells or PMA (15 ng/mL) plus calcium ionophore A23187 (Ion) (1 μM). (*A*) Transcriptional activity of NFAT in response to SEB (*Left*) or PMA+Ion (*Right*). (*B* and *C*) Transcriptional activity of an AP-1 luciferase reporter construct (*B*) and the promoter region of the RCAN1 gene (*C*) in response to PMA+Ion. Luciferase activity is represented as fold induction (observed RLU/basal RLU) over unstimulated cells (mean ± SEM). ns: nonsignificant. Results of at least two independent experiments done by triplicate are represented. (*D*) Western blot analysis of RCAN1.4 expression in extracts from Jurkat cells unstimulated or treated with PMA + Ion for 6 h in the presence or absence of OA, 10NOA (5 and 10 μM) or CsA (250 ng/mL). The figure shows non-inducible RCAN1.1 and β-Actin protein levels as loading controls. A representative experiment out of three is shown together with its corresponding normalized densitometric analysis.

NFAT by disturbing its nuclear localization, Jurkat cells transfected with hemagglutinin (HA)-tagged NFATc2 were stimulated with PMA/Ion after pretreatment with OA, 10NOA or CsA, and the cellular localization of HA-NFATc2 was analyzed by confocal fluorescence microscopy using the nucleic acid fluorescent probe TO-PRO (Fig. 4*A*). The translocation of NFATc2 to the nucleus of Jurkat cells was clearly observed upon stimulation with PMA/Ion. Interestingly, while OA did not display any significant effect on NFAT nuclear shuttling, 10NOA reduced the nuclear localization of NFATc2 to a similar extent as the CaN inhibitor CsA (Fig. 4*A*). These findings were corroborated by analyzing NFATc2 in cytoplasmic and nuclear fractions of Jurkat T cells stimulated with PMA/Ion and pretreated or not with 10NOA or CsA (Fig. 4*B*). In steady-state conditions, NFATc2 is distributed between the cytoplasmic dynamin-II- and the nuclear lamin B1-containing fractions of Jurkat cells, and upon stimulation, NFATc2 is relocalized to the nucleus (Fig. 4*B*). Interestingly, increasing concentrations of 10NOA decreased dephosphorylated NFATc2 in the nucleus and concomitantly increased phosphorylated NFATc2 in the cytoplasm (Fig. 4*B*). Similar results

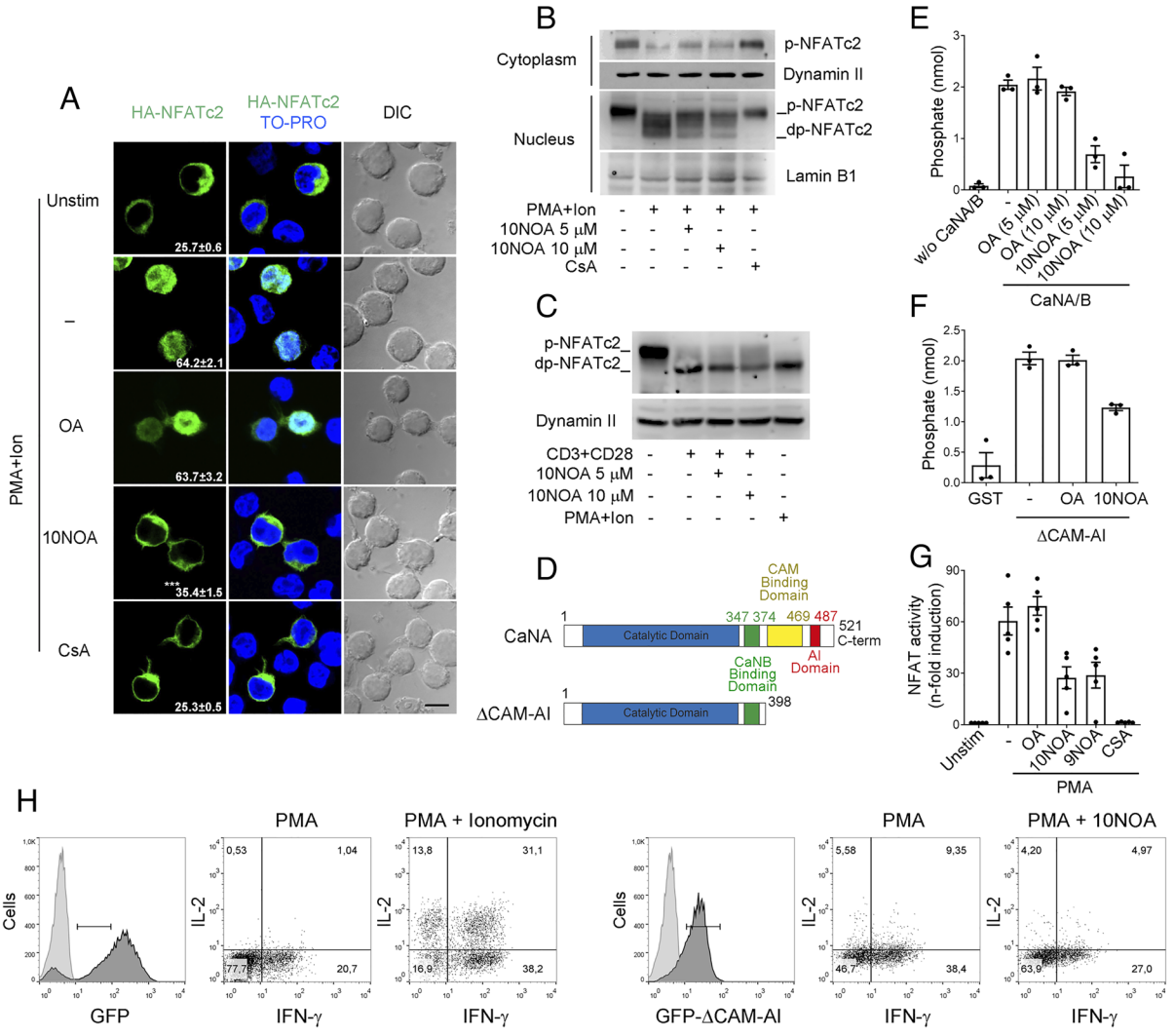

Fig. 4. 10NOA Disturbs NFAT Dephosphorylation and Nuclear Shuttling by Reducing CaN Phosphatase Activity. (*A*) Jurkat cells transfected with HA-tagged NFATc2 were left unstimulated or treated with PMA (15 ng/mL) plus calcium ionophore A23187 (Ion) (1 µM) for 2 h in the absence or presence of OA (5 µM), 10NOA (5 µM) or CsA (250 ng/mL). The localization of HA-NFATc2 was analyzed by confocal fluorescence microscopy with a primary anti-HA mAb and FITC-labeled goat anti-mouse IgG. The nucleus was stained with TO-PRO. Merged and differential interference contrast (DIC) images are shown. Percentages of HA-NFATc2 nuclear staining (mean ± SEM) from three independent experiments are indicated. ***$P < 0.001$. Bar = 15 µm. (*B*) Western blot analysis of NFATc2 in cytosolic and nuclear protein extracts from Jurkat cells pretreated or not with OA, 10NOA or CsA and incubated for 90 min with PMA + Ion. Dynamin II and Lamin B1 are shown as markers of cytosolic and nuclear cell fractions, respectively. (*C*) Western blot analysis of NFATc2 activation in total protein extracts from human T lymphoblasts stimulated with CD3/CD28 Abs and treated or not with 10NOA (5 and 10 µM) or with PMA+Ion as a control of activation. Dynamin II is shown as loading control. Phosphorylated (p-) and dephosphorylated (dp-) NFATc2 are indicated in (*B*) and (*C*). Representative experiments out of two are shown. (*D*) Structure of wild-type and ΔCAM-AI CaNA. Catalytic, CaNB binding, CAM binding and autoinhibitory (AI) domains are shown, and their delimiting amino acid residues indicated. (*E* and *F*) Phosphatase activity of recombinant CaNA (*E*) and GST-ΔCAM-AI (*F*). Before starting the reaction with the CaN phosphopeptide substrate RII, samples were pretreated for 10 min with OA or 10NOA, as indicated. Free phosphate (nmol) in each sample is represented as the mean ± SEM of three independent experiments, each one done in duplicate. (*G*) NFAT transcriptional activity of Jurkat cells co-transfected with pNFAT-LUC and the GFP-ΔCAM-AI expression vector and stimulated or not with PMA (15 ng/mL) for 6 h in the absence or presence of OA, 9NOA, 10NOA or Cyclosporine A (CsA). Luciferase activity is expressed as fold induction (mean ± SEM) of five independent experiments, each one done in triplicate. (*H*) Dot plot flow cytometry analysis showing the percentage of IL-2 and IFN-γ production in GFP-ΔCAM-AI lentiviral-transduced Th1 cells stimulated with PMA in the presence or absence of 10NOA (*Right*). GFP-transduced Th1 cells stimulated with PMA or PMA plus ionomycin are shown as controls (*Left*). Histograms also show comparable GFP expression levels of analyzed cells (3×10^3). A representative experiment out of three is shown.

were observed in total cell extracts from human T lymphoblasts stimulated with agonistic CD3/CD28 Abs. The dephosphorylation of NFATc2 in response to CD3/CD28 stimulation decreased in cells treated with increasing concentrations of 10NOA (Fig. 4*C*).

These results indicate that 10NOA inhibits NFAT translocation to the nucleus and activation in T lymphocytes by interfering with NFAT dephosphorylation.

NO_2-OA Impairs NFAT Activation Through Inhibition of CaN. The Ser/Thr phosphatase activity of CaN is largely considered key for dephosphorylation-dependent activation of NFAT in antigen-stimulated T lymphocytes (31). As NO_2-OA reduced NFAT dephosphorylation in activated T cells, we studied whether NO_2-OA could regulate NFAT activation through CaN inhibition. In vitro phosphatase assays with recombinant human CaNA (Fig. 4*D*) and CaNB, using a phospho-peptide of the RII subunit of PKA as substrate, showed that 10NOA, but not OA, reduced the phosphatase activity of CaN (Fig. 4*E*). Binding of Ca^{2+}-calmodulin (CAM) to the C-terminal region of the CaNA subunit fully activates its protein phosphatase activity by releasing the autoinhibitory region from the catalytic domain. To explore whether the inhibition exerted by 10NOA on the phosphatase activity of CaN was dependent or independent of the regulation by Ca^{2+} binding to CAM, we investigated the ability of 10NOA to inhibit a constitutively active Ca^{2+}-CAM-independent truncated form of CaNA. We used a CaNA whose C-terminal CAM-binding and autoinhibitory domains are both deleted (ΔCAM-AI) (32), but that still preserves the binding domain to the regulatory CaNB subunit (Fig. 4*D*). As observed for wild-type CaNA in the presence of CAM (Fig. 4*E*), the in vitro phosphatase activity of GST-fused ΔCAM-AI (GST-ΔCAM-AI) was reduced by 10NOA but not by OA (Fig. 4*F*). Moreover, cell-based studies confirmed that 9NOA and 10NOA, but not OA, inhibited the transcriptional activity of NFAT in Jurkat cells transfected with a GFP-fused construct of ΔCAM-AI (GFP-ΔCAM-AI) and stimulated with PMA in the absence of calcium ionophore (Fig. 4*G*). The Ca^{2+}-CAM-independent inhibition of NFAT by 10NOA was functional since, compared with GFP-expressing Th1 cells, lentiviral transduction of GFP-ΔCAM-AI promotes IL-2 and IFN-γ production in response to PMA, and 10NOA reduces their levels toward those observed in GFP-transduced Th1 cells stimulated with PMA in the absence of ionomycin (Fig. 4*H*).

These results indicate that 10NOA inhibits the protein phosphatase activity of CaNA independently of its regulation by Ca^{2+}-CAM binding, suggesting that the catalytic and/or the CaNB binding domain of CaNA may be involved.

NO_2-OA Nitroalkylates CaNA. To study whether NO_2-OA regulates the phosphatase activity of CaN by forming covalent adducts, recombinant wild-type CaNA/B, CAM, and GST-ΔCAM-AI were incubated with biotin-labeled 10NOA or OA, and nitroalkylation was detected with horseradish peroxidase (HRP)-conjugated streptavidin. Results showed that whereas OA did not bind to any of the proteins analyzed, 10NOA covalently modified both recombinant wild-type CaNA (Fig. 5*A*) and GST-ΔCAM-AI (Fig. 5*B*). In contrast, 10NOA did not bind to CAM or CaNB (Fig. 5*A*), and only trace amounts were associated with GST (Fig. 5*B*). In order to identify the amino-acid residues of CaNA that could be targets of nitroalkylation by NO_2-OA, we performed mass spectrometry studies. Recombinant CaNA incubated in vitro with 10NOA was subjected to chymotryptic digestion and nitroalkylated peptides were evaluated by high-resolution nano-HPLC-MSMS. Results showed that 10NOA covalently modified recombinant CaNA on Cys 129, 228, 266, and 372. Cys129, 228 and 266 are localized in the catalytic domain of CaNA, while Cys372 is located in the CaNB-binding domain (Fig. 5*C* and *SI Appendix*, Fig. S4). CaNA peptides bearing Cys153, 178, 184, and 256 (Fig. 5*C*) were not detected, as technical limitations impeded us from obtaining CaNA coverages higher than 85.6%.

The functional relevance of CaNA nitroalkylation was studied at the transcriptional level in Jurkat cells co-transfected with pNFAT-Luc and GFP constructs of Cys-to-Ala mutations of ΔCAM-AI on Cys129, 228, 266, or 372, as well as on the four Cys that were not detected by mass spectrometry (Fig. 5*D* and *SI Appendix*, Fig. S5 *A* and *B*). Compared with parental ΔCAM-AI, only C129A mutation was defective in mediating NFAT-dependent transcription in response to PMA stimulation (Fig. 5*D*). The close proximity of Cys129 in the α_4-helix to the active site of the catalytic domain of CaNA might partially impair its enzymatic function. Despite this, 10NOA reduced the remaining NFAT-dependent transcriptional activity of C129A to levels of parental ΔCAM-AI inhibition, and a similar reduction was observed for fully active C153A, C178A, C184A, C228A, C256A, and C266A (Fig. 5*D*). In contrast, mutation C372A made ΔCAM-AI partially resistant to inhibition by 10NOA, retaining approximately 40% of the NFAT transcriptional activity observed in ΔCAM-AI expressing cells (Fig. 5*D*). This observation was further confirmed using in vitro protein phosphatase assays, showing that only the phosphatase activity of the C372A mutant was resistant to inhibition by 10NOA (Fig. 5*E*). Moreover, covalent binding of biotinylated 10NOA to ΔCAM-AI mutants was reduced by 36 to 39% in single mutants, whereas in C372A-containing double mutants, C228A/C372A and C266A/C372A, this was further reduced to 62 and 80%, respectively (Fig. 5*F*). In order to establish that CaNA nitroalkylation of Cys372 occurs in cells, mass spectrometry-based approaches were performed. GFP immunoprecipitations from Jurkat cells expressing GFP-ΔCAM-AI and treated with 10NOA showed nitroalkylation of CaNA on Cys372 (*SI Appendix*, Fig. S6*A*). Interestingly, nitroalkylation of Cys372 was also detected on endogenous CaNA from untransfected Jurkat cells treated with either 9NOA or 10NOA (*SI Appendix*, Fig. S6 *B–E*), pointing to this Cys as the main functional target of NO_2-OA-mediated nitroalkylation of CaN in T cells.

Nitroalkylation of CaNA on Cys372 Disrupts CaNA/B Heterodimer Formation. Since Cys372 is localized within the CaNB-binding domain of CaNA, and binding of the regulatory CaNB subunit to CaNA has been demonstrated to be essential for its catalytic activity in vitro e in vivo (33, 34), we next studied whether nitroalkylation on Cys372 may interfere with functional CaNA/B heterodimer formation. Co-immunoprecipitation experiments in Jurkat cells pretreated with 10NOA reduced the amount of CaNB co-precipitated with CaNA in comparison to non-treated or OA-treated cells (Fig. 6*A*). These results were confirmed in vitro by pull-down binding assays between recombinant His_6-CaNB and GST-ΔCAM-AI. Compared with non-treated or OA-pretreated ΔCAM-AI, 10NOA reduced the binding of CaNB to ΔCAM-AI by a fourth and two-thirds, respectively (Fig. 6*B*). Moreover, the interaction between CaNA and CaNB was reduced by 10NOA in a dose-dependent manner and persists for at least 60 min (*SI Appendix*, Fig. S7 *A* and *B*). To determine the

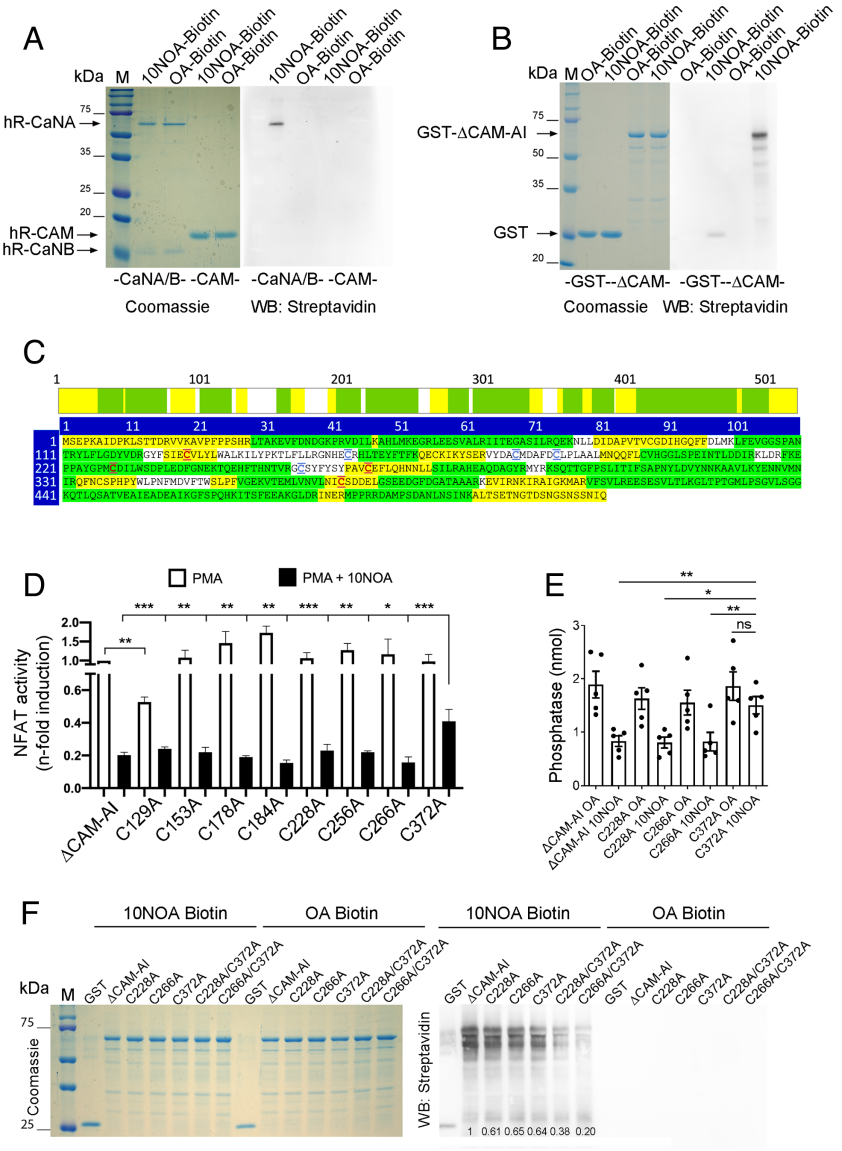

Fig. 5. 10NOA Covalently Modifies and Inhibits CaNA. (*A* and *B*) Binding of biotinylated OA and 10NOA to recombinant human CaNA, CaNB and CAM (in *A*) or GST-ΔCAM-AI (in *B*). Protein samples were incubated for 30 min with OA-Biotin or 10NOA-Biotin (5 μM). The incubation mixtures were subjected to SDS-PAGE and protein nitroalkylation was detected by western blot with HRP-conjugated streptavidin. Coomassie blue staining of gels is also shown. GST was used as control in (*B*). (*C*) Mass spectrometry-based analysis of recombinant human CaNA nitroalkylation by 10NOA. The schematic representation of CaNA shows: Chymotrypsin-digested peptide sequence matching for protein identification (85% coverage; green: 1% FDR and yellow: 5% FDR), non-covered protein sequence (white), 10NOA nitroalkylation on Cys129, 288, 266 and 372 (red) and non-detected Cys153, 178, 184, and 256 (blue). (*D*) NFAT transcriptional activity of Jurkat cells co-transfected with the pNFAT-LUC reporter and GFP-ΔCAM-AI, C129A, C153A, C178A, C184A, C228A, C256A, C266A or C372A expression vectors and stimulated with PMA (15 ng/mL) for 6 h in the presence or absence of 10NOA. Luciferase activity is expressed as fold induction normalized to luciferase activity in PMA-stimulated cells expressing parental GFP-ΔCAM-AI. Data represent the mean±SEM of three independent experiments, each one done at least twice. **P*< 0.05; ***P* < 0.01; ****P* < 0.001. (*E*) Phosphatase activity of GST-ΔCAM-AI and the Cys-to-Ala GST-ΔCAM-AI mutants C228A, C266A, and C372A, pretreated for 10 min with OA or 10NOA. Data represent the mean±SEM of five independent experiments, each one done in duplicate. **P*< 0.05; ***P* < 0.01; ns: non-significant. (*F*) In vitro binding assay of biotinylated OA or 10NOA to GST, GST-ΔCAM-AI, or the indicated GST-ΔCAM-AI Cys-to-Ala mutants. *Left* panel shows Coomassie blue staining of the analyzed proteins. *Right* panel shows HRP-streptavidin detection of nitroalkylated proteins. Normalized densitometric quantification of 10NOA-labelled samples with respect to GST-ΔCAM-AI is shown at the bottom of each lane. Data shown are representative of three independent experiments.

involvement of Cys nitroalkylation in the interference of the association between CaNA and CaNB, we performed in vitro pull-down binding assays between recombinant GST-ΔCAM-AI, C228A, C266A or C372A and His_6-tagged CaNB in the presence or absence of 10NOA (Fig. 6*C*). In the absence of 10NOA, all tested Cys-to-Ala ΔCAM-AI mutants bound CaNB to a similar extent than parental ΔCAM-AI. Noticeably, only the C372A mutant retained up to 68 % of its ability to bind to CaNB in the presence of 10NOA (Fig. 6*C*). The importance of Cys372 nitroalkylation to regulate the interaction between CaNA and CaNB observed in vitro was further confirmed in HEK293T cells co-transfected with parental GFP-ΔCAM-AI or its corresponding C372A mutant, and treated with 10NOA or OA (Fig. 6*D*). Co-immunoprecipitation experiments using anti-GFP Abs showed that mutation on Cys372 almost abrogated the inhibition of CaNB binding to ΔCAM-AI in HEK293T cells treated with 10NOA (Fig. 6*D*).

Collectively, these results strongly suggest that NO_2-OA-mediated nitroalkylation of CaNA on Cys372 interferes with the formation of functional CaNA/CaNB heterodimers, resulting in the regulation of NFAT activation and transcriptional gene expression.

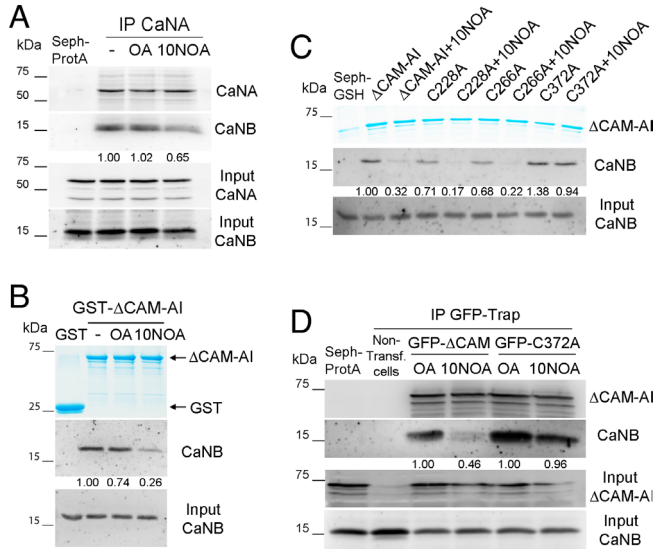

Fig. 6. 10NOA Inhibits the Binding of CaNB to CaNA. (*A*) Co-immunoprecipitation of endogenous CaNB and CaNA in 10NOA-treated Jurkat cells. Protein extracts from Jurkat cells treated with OA or 10NOA (5 μM) were immunoprecipitated with an antibody specific against CaNA or control protein A-coupled Sepharose beads (Seph-ProtA), separated by SDS-PAGE and immunoblotted with CaNA or CaNB Abs. CaNA and CaNB in cell extracts (input) are also shown. (*B*) Pull-down assay for the analysis of His_6-CaNB binding to GST or GST-ΔCAM-AI bound to GSH-Sepharose, in the presence or absence of OA or 10NOA (5 μM). *Upper* panel: Coomassie blue staining of GST and GST-ΔCAM-AI in pull-downs. *Middle* panel: Western blot for the detection of CaNB co-precipitated along with GST-ΔCAM-AI in each sample. *Lower* panel: Western blot of CaNB in cell extracts (input). (*C*) Pull-down binding assays of GSH-Sepharose-bound GST-ΔCAM-AI or its corresponding mutants C228A, C266A and C372A to His_6-CaNB in the absence or presence of 10NOA (5 μM). *Upper* panel: Coomassie blue staining showing GST-ΔCAM-AI and their corresponding Cys-to-Ala mutants in pull-downs. *Middle* panel: Western blot for the detection of CaNB co-precipitated along with the different GST-ΔCAM-AI constructs in each sample. *Lower* panel: CaNB in cell extracts (input). A representative experiment of three is shown. GSH-Sepharose was used as a control. (*D*) Analysis of the co-immunoprecipitation of CaNB with GFP-ΔCAM-AI-C372A in HEK293T cells. Extracts from HEK293T cells expressing GFP-ΔCAM-AI or GFP-ΔCAM-AI-C372A, and treated with OA or 10NOA (5 μM), were immunoprecipitated with GFP Ab-coupled Sepharose beads and separated by SDS-PAGE before western blot analysis with CaNA and CaNB Abs. *Upper* panels show GFP-ΔCAM-AI, GFP-ΔCAM-AI-C372A or CaNB in immunoprecipitates, detected by western blotting with anti-GFP or anti-CaNB specific antibodies. *Lower* panels show GFP-ΔCAM-AI, GFP-ΔCAM-AI-C372A (input-ΔCAM-AI), or CaNB (Input CaNB) detected by western blotting in cell extracts. Control lanes contain extracts from GFP-ΔCAM-AI cells incubated with Protein A-coupled Sepharose beads (Seph-ProtA) and samples from parental non-transfected HEK293T cells immunoprecipitated with GFP Ab-coupled Agarose beads. Representative western blots out of three independent experiments are shown. Normalized densitometric quantifications of CaNB binding to CaNA are depicted at the bottom of each lane.

Discussion

Our results show that NO_2-OA, but not its precursor OA, disturbs T cell proliferation. The interference of NO_2-FA in proliferation is accompanied by a decrease of CD71 on the surface of activated T cells. Interestingly, NO_2-OA also reduces the expression of both the IL-2 receptor α-chain (CD25) and its soluble cytokine ligand IL-2, which, together with CD71, are essential factors for activation-induced clonal expansion of antigen-specific T lymphocytes (35, 36). These actions of NO_2-OA on activated T cells are selective since neither the induction of the activation marker CD69 nor the viability of cells was affected. Therefore, besides the well-documented modulation that NO_2-FAs exert on the activation and proliferation of macrophages and auxiliary cells of the immune system (37–40), these bioactive lipids regulate T cell activation and proliferation. The most feasible means by which NO_2-FAs may interfere with T cell activation and proliferation is through the regulation of cytokine gene expression, which has been proposed to contribute to the resolution of inflammatory processes (11, 41). In this regard, we have shown that, besides reducing IL-2 production, NO_2-OA also inhibits IL-4 and IFN-γ synthesis in Th1 and Th2 cells and that transcriptional activation mediated by IL-4 and IFN-γ gene promoters was efficiently inhibited. Since it has been well established that IFN-γ and IL-4 foster Th1 and Th2 cell differentiation through a positive feedback mechanism that reinforces lineage stability (42, 43), one of the questions arising from our studies is whether NO_2-OA may also disturb Th1 and Th2 cell differentiation, acting on lineage-specific transcription factors such as T-bet for Th1 and STAT-6 for Th2 cells. T cell activation and differentiation require the involvement of gene transcriptional activation by NF-κB, AP-1, and NFAT (44–46), which cooperate with lineage-specific transcription factors and regulate the expression of T helper cell signature cytokines by direct binding on their gene promoter regions. Our results show that NO_2-OA inhibits NF-κB-driven transcription in T lymphocytes. The inhibition of NF-κB binding to DNA response elements and NF-κB degradation by inactivation of IκB kinase (IKK) are the main known mechanisms by which NO_2-FAs regulate NF-κB in macrophages and endothelial and tumor cells (8, 12, 47). We also observed a reduction in IκB phosphorylation and degradation by NO_2-OA in activated T cells. Therefore, NO_2-FAs may regulate NF-κB activation by inhibiting IKK in T lymphocytes, as reported in other cell types. In addition, we show here that NO_2-FAs regulate the transcriptional activity mediated by NFAT. The activation of NFAT in T cells plays an essential role in regulating genetic transcriptional programs leading to differentiation and effector functions via expression of cytokines and cytokine receptors (48). We present evidence that NO_2-OA modulates the activation of NFAT in T cells by inhibiting CaN, which reduces NFAT dephosphorylation and hence nuclear shuttling. Our results clearly show that CaN inhibition by NO_2-OA is mainly independent of regulation by Ca^{2+} binding to CAM since NO_2-OA also reduces the phosphatase and NFAT regulatory activities of ΔCAM-AI, a constitutively activated mutant of CaNA that lacks the CAM binding site (49, 50).

It is well known that NO_2-FAs are potent electrophiles that covalently modify reactive Cys thiols of many regulatory proteins (4, 51), including transcription factors and signaling molecules such as NF-κB, STING, or the Nrf2 repressor Keap1, affecting downstream gene expression and modulating oxidative and inflammatory signaling pathways (52, 53). Our studies show that CaNA is also a target for nitroalkylation by both 9NOA and 10NOA. Remarkably, in a recent unbiased high-throughput chemoproteomic study, CaNA was identified as a 9NOA target protein, validating our findings of CaNA as a relevant target of 9NOA (54). Among the 12 Cys of CaNA, we have identified four targets of nitroalkylation by NO_2-OA (Cys129, 228, 266, and 372), whereas peptides bearing Cys153, 178, 184, and 256 were not detected. Although NO_2-OA-mediated nitroalkylation of any of these four non-detected Cys cannot be completely ruled out, we found a significant reduction in the nitroalkylation of C372A-shared double mutants of CaNA, with C266A and C372A accounting for 80% of the total nitroalkylation. This reinforces the CaNA mass spectrometry data showing that these Cys are the main nucleophilic targets. Moreover, since only the Cys372 mutant was refractory to the inhibition of CaNA phosphatase activity by NO_2-OA, partially reverting its inhibitory effect on the transcriptional activity of NFAT, we conclude that nitroalkylation

on Cys372 plays a prominent role in the regulation of CaN by NO_2-OA. Notwithstanding the above, the inhibition of NFAT activation by covalent adduction of other elements downstream of CaN could not be completely ruled out as CaNA C372A did not completely reverse the inhibitory action of NO_2-OA on the transcriptional activity of NFAT.

NO_2-OA disturbs the interaction between CaNA and CaNB in vitro and in cells. The interference exerted by NO_2-OA in CaNA/CaNB heterodimer formation takes place through nitroalkylation of CaNA on Cys372, since C372A was the only nitroalkylation-sensitive CaNA mutant whose interaction with CaNB was resistant to inhibition by NO_2-OA. For optimal activity, CaNA requires interaction with CaNB (55, 56), which has become evident because, in the absence of CaNB, the CAM binding-deficient ΔCAM-AI does not dephosphorylate its substrate RII (33). Nitroalkylation of CaNA on Cys372 by NO_2-OA disturbs functional heterodimer formation between CaNA and CaNB, leading to defective NFAT-mediated transcriptional activity and cytokine production in activated T lymphocytes. This mechanism is substantially different from that reported for the immunosuppressants CsA and FK506, selective pharmacological inhibitors of CaN that prevent substrate recognition and protein phosphatase activity by forming specific complexes with immunophilins at the hydrophobic groove of the CaNA/B heterodimer interface, where they contact with the two subunits of CaN (57–59). In addition to their clinical use in preventing transplant rejection and graft-versus-host disease, CaN inhibitors have been successfully used to treat atopic dermatitis, systemic lupus erythematosus, and rheumatoid arthritis, among other autoimmune and allergic diseases (60, 61). In this sense, beneficial pharmacological actions have been reported for NO_2-FAs in well-known immune-related diseases in which T lymphocytes play an essential regulatory role such as experimental chronic inflammatory bowel disease, allergic airway inflammation, and dermatitis (7, 13, 14). This supports the concept that part of their immunoregulatory actions occur through their ability to reduce CaN/NFAT signaling, pointing to their potential as therapeutic agents for the modulation of T cell-dependent immune responses.

Altogether, our results provide additional insights into the mechanisms by which bioactive electrophilic lipids such as NO_2-OA can exert their immunomodulatory actions, namely the inhibition of NFAT signaling through the interference of the phosphatase activity of CaN. The recent systematic analyses based on the identification of CaN-binding short linear motifs have expanded the scope of proteins whose function can be regulated by the phosphatase activity of CaN, including transport by nuclear pore proteins of the NUP family (62). In this regard, even though the inhibition of NFAT activation is the most accepted mechanism by which CsA and FK506 exert their immunosuppressive actions, recent findings have shown that they may also foster immunosuppression by interfering with CaN-mediated dephosphorylation of Lck on Ser59 (63), an amino-acid residue key for Lck-triggered activation of proximal TCR signaling and integrin-mediated cytotoxicity. Whether NO_2-FAs may also regulate CaN-dependent signaling pathways other than those leading to NFAT activation deserves further investigation.

Materials and Methods

Further information is presented in *SI Appendix*.

Antibodies, Reagents, and Cells. Antibodies and reagents were sourced as follows: CD3ε OKT3 and CD28 mAbs (BioLegend); CD25-FITC, CD25-PE, and IL-2-PE (BD Biosciences); CD69-APC (ImmunoStep); IL4-PE and IFN-γ-APC mAbs (Immunotools); β-actin, CaNA (PP2B-Aα), CaNB (PP2B-B1/2), Lamin B1, HA, HSP90 and Dynamin II mAbs (Santa Cruz Biotech); GFP rAb (Merck); GFP-Trap® agarose (Chromotek); FITC-labelled goat anti-mouse IgG (DAKO); HRP-labelled donkey anti-mouse (GE Healthcare Life Sciences); goat anti-rabbit IgG (Pierce); IL-4 and IFN-γ neutralizing mAbs (R&D system); IκB and phospho-IκB mAbs (Cell Signaling); CD71 mAb was from Dr. B. Alarcón (Centro de Biología Molecular Severo Ochoa, Madrid, Spain); NFATc2 (672) pAb was from Dr. J.M. Redondo (Centro Nacional de Investigaciones Cardiovasculares, Madrid, Spain).

Recombinant human IL-2, IL-4, and IL-12 (Immunotools); streptavidin-HRP, paraformaldehyde, phytohemagglutinin (PHA), PMA, calcium ionophore A23187 and ionomycin (Sigma-Aldrich); Quick Coomasie Stain (NeoBiotech); 9NOA, 10NOA, OA and OA-Biotin (Cayman Chemicals); 10NOA-Biotin was obtained as described (8); Cyclosporine A (Calbiochem) and To-Pro-3 (Thermo Fisher).

The Raji lymphoblastoid B cell line and Jurkat T cells were grown in RPMI 1640 medium supplemented with 8% FBS (HyClone). TCRvβ3-expressing CH7C17 Jurkat T cells were grown in the presence of hygromycin (400 μg/mL) and puromycin (4 μg/mL) (Invivogen). Human peripheral blood lymphocytes used in this study were isolated from buffy coats from anonymized healthy donors (provided by Centro de Transfusiones de la Comunidad de Madrid) by separation on a biocoll gradient (Biochrom). After a 30-min plating step at 37 °C, non-adherent cells were collected and cultured for 36 h in the presence of PHA (5 μg/mL) to induce lymphocyte proliferation. To obtain T lymphoblasts, IL-2 (50 U/mL) was added to the culture medium every 2 d. All experimental procedures involving primary human T cells were approved by the Ethics Committee of the Centro Nacional de Biotecnología-Centro de Biología Molecular Severo Ochoa).

Luciferase Reporter Assay. Jurkat and CH7C17 T cells (12×10^6) were transfected with different luciferase-coupled DNA constructs (25 μg) by electroporation (350 V, 1,000 μF and 400 Ω) in 0.4 cm cuvettes, using the Gene pulser II System (Bio-Rad Laboratories). After 24 h, cells were treated for 1 h with NO_2-OA or CsA before stimulation. Jurkat cells were stimulated with PMA (15 ng/mL) and calcium ionophore A23187 (1 μM) (PMA/Ion) for 6 h. CH7C17 T cells were stimulated by conjugation with SEB-pulsed Raji APC (0.5 μg/mL) at 4:1 cell ratio and centrifuged at 120 g for 15 s to promote T cell-APC interactions. For co-transfection assays, cells were first transfected with the corresponding luciferase reporter plasmid and then transfected again 18 h later with expression plasmids of the different proteins of interest. Twenty hours post-transfection, cells were treated with different stimuli. Luciferase activity of cell extracts was determined by using a luciferase assay kit (Promega) with a luminometer Monolight 2010 (Analytical Luminescence Laboratory), and is represented as mean ± SEM fold induction (observed experimental RLUs/basal RLUs in the absence of any stimulus) or percentages with respect to stimulated cells. Transfection experiments were performed either in duplicate or triplicate.

CaN Phosphatase Activity Assay. CaN phosphatase activity was determined with the CaN Phosphatase Assay Kit (Enzo) following the provider's instructions. Briefly, diluted CAM in assay buffer (50 mM Tris, pH 7.5, 100 mM NaCl, 6 mM $MgCl_2$, 0.5 mM DTT, 0.025% NP-40, 0.5 mM $CaCl_2$) was combined with CaNA/B and OA or 10NOA (5 μM) in a microtiter plate. After 10 min, the reaction was started by adding phosphopeptide substrate RII (0.15 mM). After incubation at 37 °C for 40 min, the reaction was stopped by adding 100 μL of BIOMOL green reagent, color developed for 20 to 30 min and then plates were read at OD_{620nm} on a microplate reader absorbance iMark (Bio-Rad). When the phosphatase activity of recombinant GST-ΔCaM-AI was assayed, the reactions were done in the presence of 50 mM TrisHCl, pH 7.4, 0.5 mM $CaCl_2$, 6 mM $MgCl_2$, $MnCl_2$ 0.5 mM, 0.5 mM DTT, 0.1 μM CaN subunit B (Sinobiological) and 0.15 mM phosphorylated RII peptide.

Nitroalkylation Detection. Studies of nitroalkylation with biotinylated NO_2-OA were performed similarly as previously described (8). In brief, recombinant proteins were incubated for 60 min at 37 °C in 50 mM phosphate buffer in the presence of 1 mM EDTA and 5 μM of biotinylated 10NOA or biotinylated OA. After incubations, Laemmli sample buffer in the presence of (tris(2-carboxyethyl) phosphine) (TCEP) 5 mM was added and proteins were separated by SDS-PAGE. Inputs were detected by Coomassie staining and biotinylated proteins by western blotting with Streptavidin-HRP (Sigma-Aldrich).

Data, Materials, and Software Availability. All study data are included in the article and/or *SI Appendix*. The manuscript raw data from which all the analysis and paper results have been generated, are available at the institutional DIGITAL-CSIC repository with the dataset identifier https://doi.org/10.20350/digitalCSIC/14780.

ACKNOWLEDGMENTS. We are grateful to Noa Martín-Cófreces for input and reagents used in this study, to Ana Renshaw for her technical assistance, and to those who have helped us with different reagents as mentioned in *Materials*. Optical microscopy and flow cytometry have been conducted at the Confocal Microscopy and the Flow Cytometry Units of the Centro de Biología Molecular Severo Ochoa (CBMSO). We also thank the Genomics and Massive Sequencing Unit of the CBMSO for helpful technical assistance. This work was supported by grant RTI2018-100815-B-I00 Ministerio de Ciencia e Innovación (MICIU)/Fondo Europeo de Desarrollo Regional (FEDER) and the accompanying 2021 CSIC Exceptional Grant to M.A.Í. and J.M.S. Additional funding was obtained from grants PID2021-122348NB-I00 (MICIU) and "La Caixa" Banking Foundation (HR22-00253) to E.C. and J.V., R01GM125944-05 and DK112854-04 to F.J.S., and from Universidad de la República Comisión Intersectorial de Investigación Científica Grupos_2018, Espacio Interdisciplinario_2020 to R.R. The CBMSO receives an institutional grant from the Fundación Ramón Areces.

Author affiliations: [a]Immune System Development and Function Unit, Centro de Biología Molecular "Severo Ochoa," Consejo Superior de Investigaciones Científicas-Universidad Autónoma de Madrid, Madrid 28049, Spain; [b]Centro de Investigación Biomédica en Red de Enfermedades Cardiovasculares, Madrid 28029, Spain; [c]Laboratorio de Proteómica Cardiovascular, Centro Nacional de Investigaciones Cardiovasculares, Madrid 28029, Spain; [d]Department of Medical Biochemistry and Biophysics, Division of Vascular Biology, Karolinska Institutet, Stockholm 17177, Sweden; [e]Department of Pharmacology and Chemical Biology, University of Pittsburgh, Pittsburgh, PA 15213, USA; [f]Departamento de Bioquímica, Facultad de Medicina, Universidad de la República, Montevideo 11800, Uruguay; [g]Centro de Investigaciones Biomédicas, Facultad de Medicina, Universidad de la República, Montevideo 11800, Uruguay; [h]Departamento de Biología Molecular, Universidad Autónoma de Madrid, Madrid 28049, Spain; [i]Instituto Universitario de Biología Molecular, Universidad Autónoma de Madrid, Madrid 28049, Spain; and [j]Instituto de Investigación Sanitaria La Princesa, Madrid 28006, Spain

Author contributions: J.M.S. and M.A.Í. designed research; Á.B., M.L.C., A.G., E.C., and A.Q. performed research; F.J.S. contributed new reagents/analytic tools; Á.B., E.C., J.V., F.J.S., R.R., J.M.S., and M.A.Í. analyzed data; F.J.S. provided input into the project; R.R. provided input into the project; and Á.B., J.M.S., and M.A.Í. wrote the paper.

Competing interest statement: The authors have organizational affiliations to disclose, F.J.S. has financial interest in Creegh Pharma Inc and Furanica Inc. F.J.S. is in the board of directors of Creegh Pharma Inc and Furanica Inc., the authors have stock ownership to disclose, F.J.S. has stock in Creegh Pharma Inc and Furanica Inc., the authors have patent filings to disclose, F.J.S. has patents using nitroalkenes as therapeutic agents.

1. M. Delmastro-Greenwood, B. A. Freeman, S. G. Wendell, Redox-dependent anti-inflammatory signaling actions of unsaturated fatty acids. *Annu. Rev. Physiol.* **76**, 79–105 (2014).
2. F. J. Schopfer, N. K. H. Khoo, Nitro-fatty acid logistics: Formation, biodistribution, signaling, and pharmacology. *Trends Endocrinol. Metab.* **30**, 505–519 (2019).
3. H. Rubbo *et al.*, Nitric oxide regulation of superoxide and peroxynitrite-dependent lipid peroxidation. Formation of novel nitrogen-containing oxidized lipid derivatives. *J. Biol. Chem.* **269**, 26066–26075 (1994).
4. L. Turell, M. Steglich, B. Alvarez, The chemical foundations of nitroalkene fatty acid signaling through addition reactions with thiols. *Nitric Oxide* **78**, 161–169 (2018).
5. F. J. Schopfer *et al.*, Covalent peroxisome proliferator-activated receptor gamma adduction by nitro-fatty acids: Selective ligand activity and anti-diabetic signaling actions. *J. Biol. Chem.* **285**, 12321–12333 (2010).
6. E. Kansanen *et al.*, Electrophilic nitro-fatty acids activate NRF2 by a KEAP1 cysteine 151-independent mechanism. *J. Biol. Chem.* **286**, 14019–14027 (2011).
7. P. Wang *et al.*, Electrophilic nitro-fatty acids suppress psoriasiform dermatitis: STAT3 inhibition as a contributory mechanism. *Redox Biol.* **43**, 101987 (2021).
8. C. C. Woodcock *et al.*, Nitro-fatty acid inhibition of triple-negative breast cancer cell viability, migration, invasion, and tumor growth. *J. Biol. Chem.* **293**, 1120–1137 (2018).
9. A. J. Deen *et al.*, Regulation of stress signaling pathways by nitro-fatty acids. *Nitric Oxide* **78**, 170–175 (2018).
10. P. R. Baker, F. J. Schopfer, V. B. O'Donnell, B. A. Freeman, Convergence of nitric oxide and lipid signaling: Anti-inflammatory nitro-fatty acids. *Free Radic Biol. Med.* **46**, 989–1003 (2009).
11. N. K. H. Khoo, F. J. Schopfer, Nitrated fatty acids: From diet to disease. *Curr. Opin. Physiol.* **9**, 67–72 (2019).
12. T. Cui *et al.*, Nitrated fatty acids: Endogenous anti-inflammatory signaling mediators. *J. Biol. Chem.* **281**, 35686–35698 (2006).
13. A. T. Reddy *et al.*, The nitrated fatty acid 10-nitro-oleate attenuates allergic airway disease. *J. Immunol.* **191**, 2053–2063 (2013).
14. A. R. Mathers *et al.*, Electrophilic nitro-fatty acids suppress allergic contact dermatitis in mice. *Allergy* **72**, 656–664 (2017).
15. L. Villacorta *et al.*, Electrophilic nitro-fatty acids inhibit vascular inflammation by disrupting LPS-dependent TLR4 signalling in lipid rafts. *Cardiovasc. Res.* **98**, 116–124 (2013).
16. A. T. Reddy *et al.*, Endothelial cell peroxisome proliferator-activated receptor gamma reduces endotoxemic pulmonary inflammation and injury. *J. Immunol.* **189**, 5411–5420 (2012).
17. S. Borniquel, E. A. Jansson, M. P. Cole, B. A. Freeman, J. O. Lundberg, Nitrated oleic acid up-regulates PPARgamma and attenuates experimental inflammatory bowel disease. *Free Radic Biol. Med.* **48**, 499–505 (2010).
18. T. K. Rudolph *et al.*, Nitro-fatty acids reduce atherosclerosis in apolipoprotein E-deficient mice. *Arterioscler. Thromb. Vasc. Biol.* **30**, 938–945 (2010).
19. A. L. Hansen *et al.*, Nitro-fatty acids decrease type I interferons and monocyte chemoattractant protein 1 in ex vivo models of inflammatory arthritis. *BMC Immunol.* **22**, 77 (2021).
20. A. Koudelka *et al.*, Fatty acid nitroalkene reversal of established lung fibrosis. *Redox Biol.* **50**, 102226 (2022).
21. F. J. Schopfer, D. A. Vitturi, D. K. Jorkasky, B. A. Freeman, Nitro-fatty acids: New drug candidates for chronic inflammatory and fibrotic diseases. *Nitric Oxide* **79**, 31–37 (2018).
22. J. E. Smith-Garvin, G. A. Koretzky, M. S. Jordan, T cell activation. *Annu. Rev. Immunol.* **27**, 591–619 (2009).
23. J. Zhu, H. Yamane, W. E. Paul, Differentiation of effector CD4 T cell populations. *Annu. Rev. Immunol.* **28**, 445–489 (2010).
24. A. Rao, C. Luo, P. G. Hogan, Transcription factors of the NFAT family: Regulation and function. *Annu. Rev. Immunol.* **15**, 707–747 (1997).
25. A. Kiani *et al.*, Regulation of interferon-gamma gene expression by nuclear factor of activated T cells. *Blood* **98**, 1480–1488 (2001).
26. K. S. Ullman, J. P. Northrop, C. L. Verweij, G. R. Crabtree, Transmission of signals from the T lymphocyte antigen receptor to the genes responsible for cell proliferation and immune function: The missing link. *Annu. Rev. Immunol.* **8**, 421–452 (1990).
27. G. R. Crabtree, N. A. Clipstone, Signal transmission between the plasma membrane and nucleus of T lymphocytes. *Annu. Rev. Biochem.* **63**, 1045–1083 (1994).
28. T. Minami, Calcineurin-NFAT activation and DSCR-1 auto-inhibitory loop: How is homoeostasis regulated? *J. Biochem.* **155**, 217–226 (2014).
29. H. Li, A. Rao, P. G. Hogan, Interaction of calcineurin with substrates and targeting proteins. *Trends Cell Biol.* **21**, 91–103 (2011).
30. G. R. Crabtree, Generic signals and specific outcomes: Signaling through Ca2+, calcineurin, and NF-AT. *Cell* **96**, 611–614 (1999).
31. G. R. Crabtree, E. N. Olson, NFAT signaling: Choreographing the social lives of cells. *Cell* **109**, S67–S79 (2002).
32. S. J. O'Keefe, J. Tamura, R. L. Kincaid, M. J. Tocci, E. A. O'Neill, FK-506- and CsA-sensitive activation of the interleukin-2 promoter by calcineurin. *Nature* **357**, 692–694 (1992).
33. Q. Wei, E. Y. Lee, Mutagenesis of the L7 loop connecting beta strands 12 and 13 of calcineurin: Evidence for a structural role in activity changes. *Biochemistry* **36**, 7418–7424 (1997).
34. I. A. Graef, F. Chen, L. Chen, A. Kuo, G. R. Crabtree, Signals transduced by Ca(2+)/calcineurin and NFATc3/c4 pattern the developing vasculature. *Cell* **105**, 863–875 (2001).
35. M. Reddy, E. Eirikis, C. Davis, H. M. Davis, U. Prabhakar, Comparative analysis of lymphocyte activation marker expression and cytokine secretion profile in stimulated human peripheral blood mononuclear cell cultures: An in vitro model to monitor cellular immune function. *J. Immunol. Methods* **293**, 127–142 (2004).
36. M. Shipkova, E. Wieland, Surface markers of lymphocyte activation and markers of cell proliferation. *Clin. Chim. Acta* **413**, 1338–1349 (2012).
37. H. Verescakova *et al.*, Nitro-oleic acid regulates growth factor-induced differentiation of bone marrow-derived macrophages. *Free Radic. Biol. Med.* **104**, 10–19 (2017).
38. L. Villacorta *et al.*, Nitro-linoleic acid inhibits vascular smooth muscle cell proliferation via the Keap1/Nrf2 signaling pathway. *Am. J. Physiol. Heart Circ. Physiol.* **293**, H770–H776 (2007).
39. G. Ambrozova *et al.*, Nitro-oleic acid inhibits vascular endothelial inflammatory responses and the endothelial-mesenchymal transition. *Biochim. Biophys. Acta* **1860**, 2428–2437 (2016).
40. K. Panati *et al.*, The nitrated fatty acid, 10-nitrooleate inhibits the neutrophil chemotaxis via peroxisome proliferator-activated receptor gamma in CLP-induced sepsis in mice. *Int. Immunopharmacol.* **72**, 159–165 (2019).
41. M. Piesche *et al.*, The emerging therapeutic potential of nitro fatty acids and other Michael acceptor-containing drugs for the treatment of inflammation and cancer. *Front Pharmacol.* **11**, 1297 (2020).
42. R. B. Smeltz, J. Chen, R. Ehrhardt, E. M. Shevach, Role of IFN-gamma in Th1 differentiation: IFN-gamma regulates IL-18R alpha expression by preventing the negative effects of IL-4 and by inducing/maintaining IL-12 receptor beta 2 expression. *J. Immunol.* **168**, 6165–6172 (2002).
43. L. Chen *et al.*, IL-4 induces differentiation and expansion of Th2 cytokine-producing eosinophils. *J. Immunol.* **172**, 2059–2066 (2004).
44. S. Paul, B. C. Schaefer, A new look at T cell receptor signaling to nuclear factor-kappaB. *Trends Immunol.* **34**, 269–281 (2013).
45. J. U. Lee, L. K. Kim, J. M. Choi, Revisiting the concept of targeting NFAT to control T cell immunity and autoimmune diseases. *Front. Immunol.* **9**, 2747 (2018).
46. F. Macian, C. Lopez-Rodriguez, A. Rao, Partners in transcription: NFAT and AP-1. *Oncogene* **20**, 2476–2489 (2001).
47. L. Villacorta *et al.*, In situ generation, metabolism and immunomodulatory signaling actions of nitro-conjugated linoleic acid in a murine model of inflammation. *Redox Biol.* **15**, 522–531 (2018).
48. N. Hermann-Kleiter, G. Baier, NFAT pulls the strings during CD4+ T helper cell effector functions. *Blood* **115**, 2989–2997 (2010).
49. A. Kawamura, M. S. Su, Interaction of FKBP12-FK506 with calcineurin A at the B subunit-binding domain. *J. Biol. Chem.* **270**, 15463–15466 (1995).
50. J. N. Parsons *et al.*, Regulation of calcineurin phosphatase activity and interaction with the FK-506. FK-506 binding protein complex. *J. Biol. Chem.* **269**, 19610–19616 (1994).
51. V. Grippo *et al.*, Electrophilic characteristics and aqueous behavior of fatty acid nitroalkenes. *Redox Biol.* **38**, 101756 (2021).
52. T. Melo, J. F. Montero-Bullon, P. Domingues, M. R. Domingues, Discovery of bioactive nitrated lipids and nitro-lipid-protein adducts using mass spectrometry-based approaches. *Redox Biol.* **23**, 101106 (2019).
53. A. L. Hansen *et al.*, Nitro-fatty acids are formed in response to virus infection and are potent inhibitors of STING palmitoylation and signaling. *Proc. Natl. Acad. Sci. U.S.A.* **115**, E7768–E7775 (2018).
54. M. Y. Fang *et al.*, Chemoproteomic profiling reveals cellular targets of nitro-fatty acids. *Redox Biol.* **46**, 102126 (2021).
55. S. J. Li *et al.*, Cooperative autoinhibition and multi-level activation mechanisms of calcineurin. *Cell Res.* **26**, 336–349 (2016).

56. J. Rumi-Masante *et al.*, Structural basis for activation of calcineurin by calmodulin. *J. Mol. Biol.* **415**, 307–317 (2012).
57. H. Ke, Q. Huai, Structures of calcineurin and its complexes with immunophilins-immunosuppressants. *Biochem. Biophys. Res. Commun.* **311**, 1095–1102 (2003).
58. L. Jin, S. C. Harrison, Crystal structure of human calcineurin complexed with cyclosporin A and human cyclophilin. *Proc. Natl. Acad. Sci. U.S.A.* **99**, 13522–13526 (2002).
59. A. Rodriguez *et al.*, A conserved docking surface on calcineurin mediates interaction with substrates and immunosuppressants. *Mol. Cell* **33**, 616–626 (2009).
60. J. M. Hanifin, M. R. Ling, R. Langley, D. Breneman, E. Rafal, Tacrolimus ointment for the treatment of atopic dermatitis in adult patients: Part I, efficacy. *J. Am. Acad. Dermatol.* **44**, S28–S38 (2001).
61. Y. J. Park, S. A. Yoo, M. Kim, W. U. Kim, The role of calcium-calcineurin-NFAT signaling pathway in health and autoimmune diseases. *Front. Immunol.* **11**, 195 (2020).
62. C. P. Wigington *et al.*, Systematic discovery of short linear motifs decodes calcineurin phosphatase signaling. *Mol. Cell* **79**, 342–358.e312 (2020).
63. S. Otsuka *et al.*, Calcineurin inhibitors suppress acute graft-versus-host disease via NFAT-independent inhibition of T cell receptor signaling. *J. Clin. Invest.* **131**, e147683 (2021).